Effect of Solvent Quality on the Level of Association and Encounter Kinetics of Hydrophobic Pendants Covalently Attached onto a Water-Soluble Polymer

Sabesh Kanagalingam, Crystal F. Ngan, and Jean Duhamel*

Institute for Polymer Research, Department of Chemistry, University of Waterloo, 200 University Avenue West, Waterloo, ON N2L 3G1, Canada

Received May 15, 2002; Revised Manuscript Received July 26, 2002

ABSTRACT: Pyrene-labeled poly(*N*,*N*-dimethylacrylamide)s were prepared by radical copolymerization of *N*,*N*-dimethylacrylamide with *N*-(1-pyrenylmethyl)acrylamide. The progress of the copolymerization reaction was followed by ^{1}H NMR to ensure that the pyrene-labeled monomer was homogeneously incorporated into the polymer backbone. Since pyrene is hydrophobic and poly(*N*,*N*-dimethylacrylamide) is water-soluble, a set of water-soluble associative polymers was generated. The effect of solvent quality toward these associative polymers was investigated. The level of association and the kinetics of encounter between pendants were determined in *N*,*N*-dimethylformamide (DMF), acetone, water, and mixtures of acetone and water. Analysis of the fluorescence decays with a blob model yields quantitative results which agree with the qualitative information retrieved by other techniques (static light scattering, intrinsic viscosity, UV−vis absorption). The level of association between hydrophobic pendants was found to be small in acetone (a good solvent for pyrene). It increases when water is added to the solution, since pyrene is insoluble in water. The level of association is smaller in DMF than in acetone, because DMF is a better solvent than acetone for the polymer, and swelling of the polymer coil results in a decrease of the interactions existing between the pyrene groups.

Introduction

Interesting viscoelastic properties exhibited by solutions of associating polymers (AP) have rendered them useful in a multitude of industrial applications, such as associative thickeners in paints, drag reducing agents in pipelines, oil recovery agents or viscosity modifiers in oil.[1] Characterizing APs' associative behavior has been the subject of intensive study. APs are typically made of a backbone soluble in a given solvent onto which insoluble units have been attached. The intermolecular associations between insoluble pendants form a transient network resulting in highly viscous solutions.[2] The micellelike aggregates made of insoluble moieties constitute the keystones of the AP network.[3] In many cases, the intermolecular cross-linkages are severed under shear and the viscosity plummets.[4] The ability of AP solutions to shear-thin has led to numerous practical applications. Since the desirable viscoelastic behavior of APs is due to their associating power, methodologies are required that can provide information about the fraction of insoluble pendants which are associated. We refer to this parameter as the level of association (f_{agg}).

Over the last 5 years, our laboratory has developed such a methodology for APs where the dye pyrene is either the associating group or is covalently attached onto the associating group and is randomly distributed along the polymer backbone.[5] The reason for using pyrene as a probe for the associative pendant arises from its ability to form excimers.[6] Upon photon absorption, an excited pyrene can either fluoresce or encounter a ground-state pyrene via diffusion to form an excited complex called an excimer. An excimer can also be generated instantaneously when aggregated pyrenes absorb a photon. Careful analysis of the fluorescence data can distinguish whether the excimer is formed instantaneously or by diffusion. The determination of the fractions of pyrenes which either form excimer by diffusion or are involved in a pyrene aggregate yields the level of association of a given pyrene-labeled AP.[5]

So far, this methodology has been applied to determine the level of association of two pyrene-labeled APs, namely a maleated ethylene propylene copolymer[5a] and a hydrophobically modified alkali swellable emulsion copolymer.[5b] Each study was carried out with a limited number of pyrene-labeled polymers, the former study with just one polymer and the latter with three polymers having very low pyrene contents. Both studies established quantitatively that a better solvent for the associating pendants leads to a smaller level of association of the AP. These preliminary results encouraged us to undertake an in-depth study of a water-soluble AP to investigate the relationship existing between solvent, polymer backbone, hydrophobic content and the level of association.

To this effect, seven pyrene-labeled poly(*N*,*N*-dimethylacrylamide)s (PyPDMAAm) were synthesized by random copolymerization of *N*,*N*-dimethylacrylamide (DMAAm) with *N*-(1-pyrenylmethyl)acrylamide (PyMAAm). The incorporation of PyMAAm into the PDMAAm backbone occurred randomly as shown by ^{1}H NMR experiments carried out during the course of the polymerization (cf. Experimental Section). The pyrene content of the PyPDMAAms (called λ in mol of pyrene/g of polymer) ranged from 15 to 645 μmol/g. The pyrene content of each polymer is listed in Table 1 along with its weight-average molecular weight determined by

* To whom correspondence should be addressed.

10.1021/ma0207428 CCC: $22.00
Published on Web 09/27/2002

Scheme 1. Two-Dimensional Blob Representations of a Polymer Chain Randomly Labeled with Pyrene: (A) Polymer Coil Is Divided into Blobs: (B) Definition of Two Parameters Associated with the *Blob* Model. the Areas Shaded Dark Gray, Light Gray, and White, Are Rich, Poor, and Absent of Pyrene, Respectively

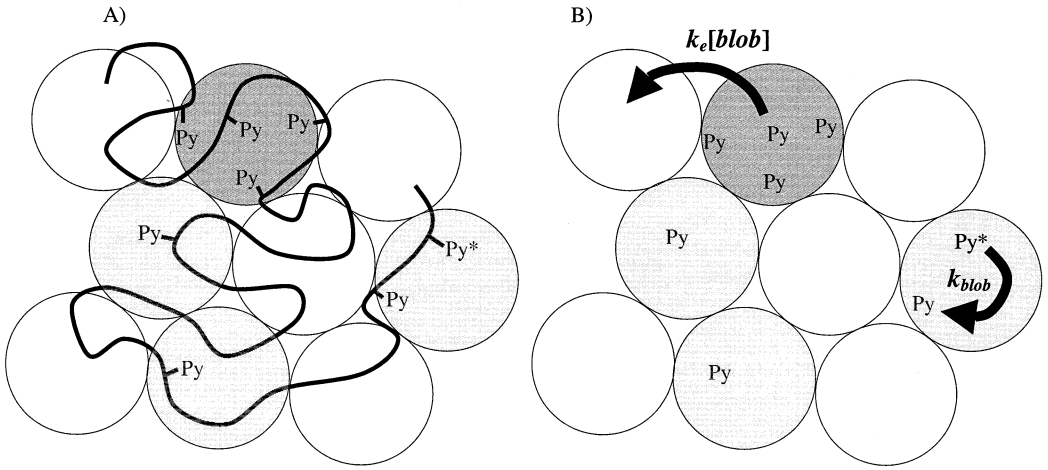

Table 1. Weight-Average Molecular Masses (Determined by Static Light Scattering), Pyrene Content in mol % and λ (mol of Pyrenes/g of Polymer) of PyPDMAAm and PDMAAm (Determined by UV−Vis Absorption)

polymer	$\overline{M_w}$, kg/mol	pyrene content, mol %	λ, μmol/g
PDMAAm	94	0.0	0
15PyPDMAAm	80	0.2	15
100PyPDMAAm	297	1.0	98
265PyPDMAAm	165	2.7	263
350PyPDMAAm	134	3.7	349
480PyPDMAAm	123	5.2	479
570PyPDMAAm	105	6.3	570
650PyPDMAAm	105	7.3	645

static light scattering. In water, PDMAAm is readily soluble, whereas pyrene is sparingly soluble. Consequently PyPDMAAm is a water-soluble AP where the associating groups are the pyrene dyes. The level of association of each PyPDMAAm was measured in solvents having different solvating abilities toward pyrene and the PDMAAm backbone. Using static light scattering, intrinsic viscosity, and UV−vis absorption measurements, the following conclusions could be drawn about the solvating abilities of *N*,*N*-dimethylformamide (DMF), acetone, and water. DMF is a good solvent for both the backbone and the pyrene moieties, acetone is a solvent which is good for pyrene and poor for the polymer backbone whereas water is a solvent which is good for the polymer backbone and bad for the pyrene moieties.

The direct effect of changing solvent is to affect how PyPDMAAm is being solvated. There is also an indirect effect which is to alter the way pendants randomly located along the polymer backbone encounter. A good solvent for the polymer backbone stretches the chain, which leads to less diffusional encounters between pendants. Since the first step in the determination of f_{agg} requires establishing the rate of diffusional encounter between pendants, the effect of solvent quality on the rate of encounter is discussed in detail in this article. This discussion is followed by the study of the effect of solvent on the f_{agg} parameter.

To the best of our knowledge, no other method in the literature can accomplish what the procedure outlined in this study does in terms of describing the diffusional encounters between pyrenes attached randomly onto a polymeric backbone under any solvent conditions. Since pyrene is coined as being "the most frequently used dye in fluorescence studies of labeled polymers",[7] this procedure is expected to provide a valuable tool for the characterization of any polymeric system which has been covalently labeled with the dye pyrene.

Theory

In this report, a blob model is used to determine quantitatively the level of association of a series of PyPDMAAms. The equations presented in this section are the final results of derivations which have been reported in earlier publications.[5b,8] To apply the blob model, the polymer coil is divided arbitrarily into theoretical blobs defined as a region of the polymer coil probed by an excited pyrene during its lifetime (cf. Scheme 1). The pyrene pendants distribute themselves randomly among the blobs according to a Poisson distribution. The blob model describes the formation of excimer by diffusion utilizing three parameters: The rate constant of excimer formation within a blob, k_{blob},[9] the rate constant at which pyrene groups exchange from blob to blob, k_e[blob] (where k_e is the exchange rate constant and [blob] is the blob concentration inside the polymer coil) and the average number of pyrene groups per blob, $\langle n \rangle$. According to the blob model, the excited pyrene monomers have a time-dependent behavior given by eq 1 where the fraction f refers to the pyrene monomers that form excimer by diffusion. The fraction $(1 - f)$ refers to the pyrenes that do not form excimer and fluoresce with their natural lifetime τ_M.

$$[\mathrm{Py}^*]_{(t)} = f \exp\left[-\left(A_2 + \frac{1}{\tau_M}\right)t - A_3(1 - \exp(-A_4 t))\right] + (1 - f)\exp(-t/\tau_M) \quad (1)$$

The parameters A_2, A_3, and A_4 are given in eq 2.

$$A_2 = \langle n \rangle \frac{k_{diff}\, k_e[\mathrm{blob}]}{k_{diff} + k_e[\mathrm{blob}]} \quad A_3 = \langle n \rangle \frac{{k_{diff}}^2}{(k_{diff} + k_e[\mathrm{blob}])^2}$$
$$A_4 = k_{diff} + k_e[\mathrm{blob}] \quad (2)$$

Scheme 2 illustrates how excimers are produced. Excimers can be formed either by diffusive encounters

Scheme 2

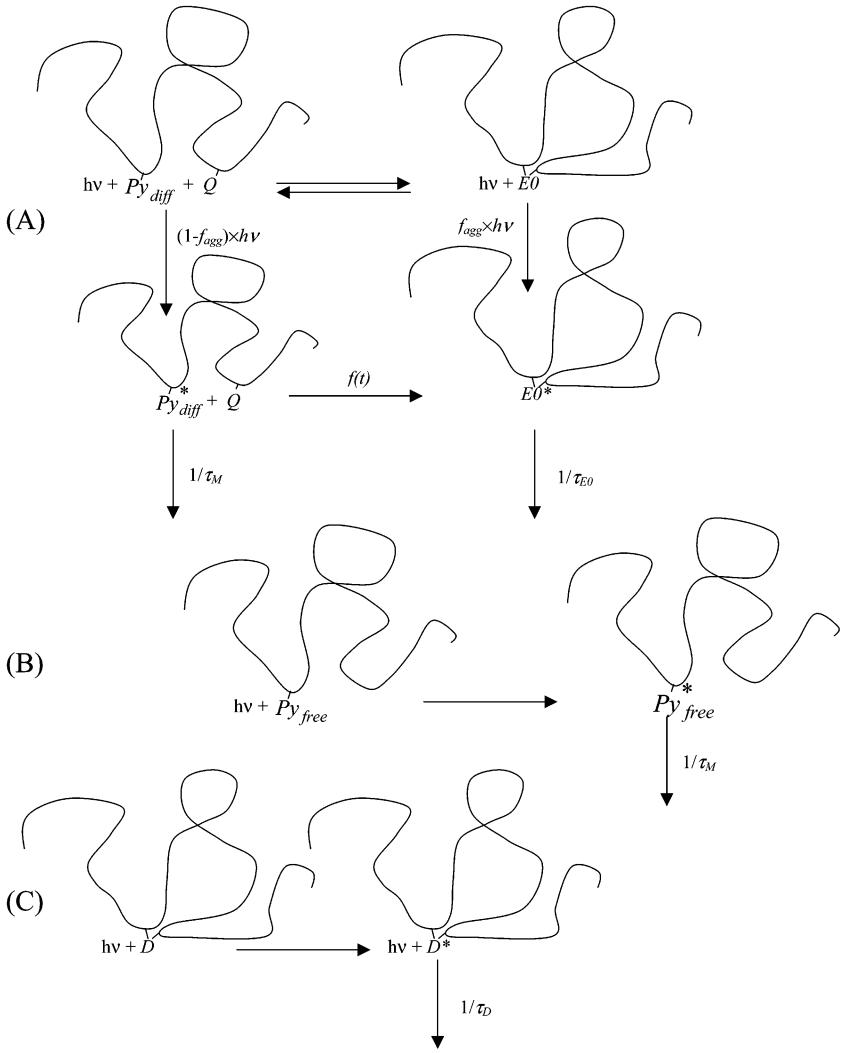

or from direct excitation of preassociated pyrenes. A fraction of pyrenes associated in the ground state (f_{agg}) absorbs a fraction of the excitation light. These form excimer instantly. The remaining fraction ($1 - f_{agg}$) of pyrenes represents nonassociated pyrenes. A fraction of them (f, introduced in eq 1) may diffusively encounter a ground-state pyrene to form an excimer. Those pyrenes are referred to as Py^*_{diff}. The remaining fraction ($1 - f$) of unassociated pyrenes characterizes those unassociated pyrenes which do not form excimer (Py^*_{free}) and fluoresce with their natural lifetime (τ_M). Because preassociated ground-state pyrenes and isolated ground-state pyrenes can both encounter the excited pyrene by diffusion to form an excimer, they are being referred to as quenchers (Q) of Py^*_{diff} in Scheme 2.

Two populations of excimer are used in Scheme 2, namely E_0* and D*. The first population, E_0*, corresponds to the excimers which exhibit the ideal $\pi-\pi$ stacking expected of traditional pyrene excimers and fluoresce with a lifetime τ_{E_0}. The second one, D*, corresponds to the excimers which are formed inside pyrene aggregates, that do not exhibit the ideal geometry of pyrene excimers and fluoresce with a longer lifetime τ_D ($\tau_D > \tau_{E_0}$). The existence of such excimers has been reported.[5,10] They are often encountered in polymeric systems where the polymer backbone restricts the freedom of the dye preventing the ideal overlap of the pyrene orbitals. Equation 3 describes the time-dependent profile of the excimer.

$$[E^*] = -[\mathrm{Py}^*_{\mathrm{diff}}]_{(t=0)} e^{-A_3} \sum_{i=0}^{\infty} \frac{A_3^{\,i}}{i!} \times \frac{\frac{1}{\tau_M} + A_2 + iA_4}{\frac{1}{\tau_M} - \frac{1}{\tau_{E_0}} + A_2 + iA_4} \exp\left(-\left(\frac{1}{\tau_M} + A_2 + iA_4\right)t\right) + \left([\mathrm{E_0}^*]_{(t=0)} + [\mathrm{Py}^*_{\mathrm{diff}}]_{(t=0)} e^{-A_3} \sum_{i=0}^{\infty} \frac{A_3^{\,i}}{i!} \times \frac{\frac{1}{\tau_M} + A_2 + iA_4}{\frac{1}{\tau_M} - \frac{1}{\tau_{E_0}} + A_2 + iA_4}\right) e^{-t/\tau_{E0}} + [\mathrm{D}^*]_{(t=0)} e^{-t/\tau_D} \quad (3)$$

The excimer fluorescence decays were fitted with eq 3, where the parameters k_{blob}, $\langle n \rangle$, and k_e[blob] have been retrieved beforehand from the analysis of

the monomer decays, and are fixed in the analysis. The analysis of the monomer decays with eq 1 combined with the analysis of the excimer decays with eq 3 yields the relative initial contributions from all four species $[Py^*_{free}]_{(t=0)}$, $[Py^*_{diff}]_{(t=0)}$, $[E_0^*]_{(t=0)}$, and $[D^*]_{(t=0)}$ and their fractions are obtained in eqs 4, parts a−d:

$$f_{diff} = \frac{[Py^*_{diff}]_{(t=0)}}{[Py^*_{diff}]_{(t=0)} + [Py^*_{free}]_{(t=0)} + [E_0^*]_{(t=0)} + [D^*]_{(t=0)}} \quad (4a)$$

$$f_{free} = \frac{[Py^*_{free}]_{(t=0)}}{[Py^*_{diff}]_{(t=0)} + [Py^*_{free}]_{(t=0)} + [E_0^*]_{(t=0)} + [D^*]_{(t=0)}} \quad (4b)$$

$$f_{E_0} = \frac{[E_0^*]_{(t=0)}}{[Py^*_{diff}]_{(t=0)} + [Py^*_{free}]_{(t=0)} + [E_0^*]_{(t=0)} + [D^*]_{(t=0)}} \quad (4c)$$

$$f_D = \frac{[D^*]_{(t=0)}}{[Py^*_{diff}]_{(t=0)} + [Py^*_{free}]_{(t=0)} + [E_0^*]_{(t=0)} + [D^*]_{(t=0)}} \quad (4d)$$

The sum of f_{E_0} and f_D yields f_{agg}, the fraction of pendants which are associated.

Experimental Section

All chemicals were purchased from Sigma-Aldrich (Milwaukee, WI) except for the ones listed below. Sodium dodecyl sulfate (SDS) was purchased from VWR (Mississauga, ON). Solvents of spectrograde quality (acetone, DMF and diethyl ether) were purchased from either Sigma-Aldrich, or VWR and used interchangeably. All solvents were used as received unless otherwise noted. The double distilled water (deionized from Millipore Milli-RO 10 Plus and Milli-Q UF Plus (Bedford, MA)) was used in all preparatory steps and spectroscopy experiments.

Synthesis of *N*-(1-Pyrenylmethyl)acrylamide (PyMAAm). The synthesis of PyMAAm was accomplished by the reaction of acryloyl chloride with 1-pyrenemethylamine hydrochloride ($PyMeNH_2$.HCl). The amine was dried under vacuum in a drying flask at 60 °C for 2 h prior to use. All reaction flasks were dried under vacuum to remove any traces of moisture. *N*-Methylmorpholine (1.3 mL, 11.8 mmol) was added using a dry, airtight syringe to a suspension of 1.081 g (4.04 mmol) of $PyMeNH_2$.HCl in 40 mL of chloroform under N_2 atmosphere. The slurry was stirred for 1 h at ∼0 °C until a thick white solution of $PyMeNH_2$ (solution A) was obtained. In a second flask, 3.0 mL (30 mmol) of acryloyl chloride was added to 10 mL of ice-cooled chloroform under N_2 atmosphere. This acryloyl chloride solution was added dropwise by a dry, airtight, N_2 flushed syringe to the ice-cold solution A. The reaction mixture was allowed to warm to room temperature over 2 h and then stirred for 24 h. A milky solution with some white precipitates was obtained. To this solution was added 50 mL of chloroform. The precipitate (*N*-methylmorpholine−HCl) was removed by filtration. The filtrate was washed twice with 0.25 N HCl, saturated NaCl, saturated $NaHCO_3$, and saturated NaCl solutions in that order. The chloroform layer was dried over anhydrous $MgSO_4$. The $MgSO_4 \cdot H_2O$ was removed by gravity filtration. The product was washed thoroughly with benzene (yield 81%), dried under vacuum and then recrystallized from chloroform. 200 MHz ^{1}H NMR ($CDCl_3$): δ 5.2 (d, 2H, Py−CH_2), 5.6 (d of d, 1H, alkene trans-H), 5.8 (m, 1H, NH), 6.1 (d of d, 1H, alkene cis-H), 6.3 (d, 1H, alkene gem-H), 7.9−8.3 (several peaks, 9H, phenyl H's). IR (solid dry film): cm^{-1} 1667 (strong) amide I band CO abs; 1550 (strong) amide II NH bending, 3275 (strong) NH stretching, 3034 (med) phenyl CH stretching. UV−vis (0.05 M SDS in water): distinctive pyrene peaks at 344 ($\epsilon = 4.3 \times 10^4$ M^{-1} cm^{-1}), 328, and 314 nm.

Random Copolymerization. The copolymers were synthesized with various comonomer mole ratios of PyMAAm to *N*,*N*-dimethylacrylamide (DMAAm). The exact pyrene content (λ, mol of pyrene/g of polymer) was determined postsynthesis by UV−vis absorption measurements. The polymerization procedures were essentially the same for all polymers that were made, and the general scheme is as follows: PyMAAm was recrystallized and dried under vacuum prior to use. DMAAm was eluted through an inhibitor remover column three times and distilled under vacuum. A dry, N_2 filled glass ampule containing 0.061 g (0.223 mmol, 1.4 mol %) of PyMAAm, 1.626 g (16.4 mmol, 98.6 mol %) of DMAAm, 0.0010 g of AIBN, and 10 mL of DMF was outgassed in a vacuum line by six freeze−thaw cycles. The solution mixture in the last two cycles was thawed to room temperature. The ampule was then sealed under vacuum. The polymerization was carried out at 58 ± 2 °C to conversions of up to 40%. The polymerization mixture was cooled to ∼0 °C and added dropwise to 10× excess ice-cold diethyl ether to precipitate the polymer. The white or light yellowish polymer was dialyzed against water with 3500 MW cutoff dialysis bag to remove oligomers, residual DMF, and unreacted monomers. The polymer solution was removed from the bag and rotovaped to remove water. The polymer was then redissolved in acetone and the polymer solution was added dropwise into 10× excess ice-cold diethyl ether until a large amount of white precipitates formed. This was repeated four more times. The precipitates were then removed and dried under vacuum for 2 days at 70 °C. 200 MHz ^{1}H NMR (acetone-d_6): δ 1.2 and 1.7 (broad, ∼2H, CH_2), 2.6 (broad merged with next peak, ∼1H, CH), 2.9 and 3.1 (s, ∼6H, NCH_3), 5.2 (broad, seen in polymers with pyrene content > 4 mol %, Py−CH_2), and 7.9−8.4 (several peaks, pyrenyl H). UV−vis (0.05 M SDS in water): distinctive pyrene peaks at 344, 328, and 314 nm. Weight-average molecular weights were obtained by static light scattering measurements.

Determination of Random Copolymerization. The random copolymerization of 91 mol % of DMAAm with 9 mol % of PyMAAm was conducted in deuterated DMF with the same procedure outlined above and followed over time by ^{1}H NMR. In a Schlenk flask were placed 0.060 g (0.21 mmol, 8.8 mol %) of PyMAAm, 0.2172 g (21.9 mmol, 91.2 mol %) of DMAAm, 0.0004 g of AIBN, and 3 mL of DMF-d_7. Several aliquots (∼20 μL) of the reaction mixture were removed over time under inert conditions and dissolved in $CDCl_3$, and a NMR spectrum was acquired on a 500 MHz Bruker spectrometer. The usage of deuterated solvent allowed for the quantitative monitoring of the peak integral associated with the various compounds in the reaction mixture, namely the polymer and the two monomers. The ^{1}H NMR spectrum at the midpoint of the reaction exhibited the following peaks: δ 1.2 and 1.7 (broad, polymer backbone CH_2), 2.6 (broad merged with next peak, polymer backbone CH), 2.9−3.1 (broad peaks, NCH_3 of polymer and DMAAm), 5.20 (d, Py−CH_2) and 7.9−8.4 (several peaks, pyrenyl H of polymer and PyDMAAm). 5.60−5.64 (two d of d, alkene trans-H of PyMAAm and DMAAm), 6.12 (d of d, alkene cis-H of PyMAAm), 6.24 (d of d, alkene gem-H of DMAAm), 6.34 (d of d, alkene gem-H of PyMAAm), 6.55 (d of d, alkene cis-H of DMAAm). The peaks at 6.55 and 6.24 ppm were chosen to determine how much DMAAm monomer was present for a given conversion. The peaks at 6.12 and 6.34 ppm were chosen to characterize the DMAAm monomer. All the peaks were observed against the internal standard pyrene (several peaks from 7.9 to 8.3 ppm). The decrease of the peak intensities of DMAAm and PyDMAAm with respect to the internal standard was monitored over time to yield the cumulative copolymer composition. Figure S1 in the Supporting Information is the plot of the cumulative copolymer composition as a function of conversion which shows no appreciable drift from the initial feed composition for monomer conversions up to 80%. This confirms that the incorporation

of 9 mol % of PyDMAAm into the copolymer is random. Consequently all polymers investigated in this study were randomly labeled with pyrene, since they all had a pyrene content lower than 9 mol %.

Pyrene Content of Copolymer Samples. A Hewlett-Packard 8452A diode array spectrophotometer was used for the absorption measurements. The spectrometer has an accuracy of at most ±1 nm. The copolymer composition was determined by UV−vis absorption measurements. The pyrene content of the polymer was established by measuring the absorption of a solution prepared from a carefully weighed amount (m_p) of pyrene labeled polymer in a known volume (V_p) of acetone solution. The pyrene concentration [Py] was then estimated from the absorption value at 344 nm in acetone (ϵ = 40,000 M^{-1} cm^{-1}). The pyrene content λ for the copolymer could be calculated from

$$\lambda = \frac{[\mathrm{Py}]}{m_p/V_p}$$

expressed in mol of pyrene/g of polymer. The polymer absorption spectra were obtained in water solutions to qualitatively determine the amount of aggregation using the peak-to-valley ratio, P_A.[7]

Light-Scattering Measurements. The absolute weight-average molecular weight of all the polymers was determined using static light-scattering measurements. Refractive index increments (dn/dc) were determined for the PDMAAm, 15-PyPDMAAm, 100-PyPDMAAm, 265-PyPDMAAm, and 645-PyPDMAAm. For all the other polymers, it was evaluated as a composition-weighted average of the values determined for these polymers.[11] The dn/dc values of the polymers were measured at 22.0 ± 0.1 °C using a Brice-Phoenix differential refractometer equipped with a 510 nm band-pass interference filter. Light-scattering measurements for PDMAAm were done in water, acetone, and DMF. Measurements of all the PyPDMAAm polymers were done in acetone and the weight-average molecular weights are reported in Table 1. Measurements for 265-PyPDMAAm, 480-PyPDMAAm, and 645-PyPDMAAm were done in DMF. A Brookhaven BI-200 SM light-scattering goniometer equipped with a Lexel 2 W argon ion laser operating at 514.5 nm was used for the static light-scattering measurements. The weight-average molecular weight was determined by Zimm extrapolation to zero angle and zero concentration for a series of measurements for six to eight solutions of concentrations between 0.1 and 1.0% (w/v) at angles ranging from 45 to 150°. The samples were filtered through 0.5 μm filters prior to light-scattering measurements.

Intrinsic Viscosity Measurements. Viscosities of the PDMAAm were measured in DMF and acetone at 20.0 ± 0.1 °C with a Ubbelohde viscometer in a water bath in order to determine intrinsic viscosity [η].

Steady-State Fluorescence Measurements. Fluorescence spectra were recorded on a Photon Technology International LS-100 steady-state system with a pulsed xenon flash lamp as the light source. The spectra of all solutions were obtained with the usual right angle configuration. All solutions were degassed under a gentle flow of nitrogen for 20 min. The samples were excited at 344 nm and the fluorescence intensities of the monomer (I_M) and of the excimer (I_E) were obtained by taking the integrals under the fluorescence spectra from 372 to 378 nm for the monomer and from 500 to 530 nm for the excimer.

Time-Resolved Fluorescence Measurements. Fluorescence decay curves were obtained by the time-correlated single photon counting technique with a Photochemical Research Associates Inc. System 2000. The excitation wavelength was set at 344 nm and the fluorescence from the pyrene monomer and excimer were monitored at 375 and 510 nm, respectively. More experimental details about this instrument can be found in earlier publications.[5,8]

Analysis of the Fluorescence Decays. The fluorescence decays were fitted by either a sum of 2, 3, or 4 exponentials (cf. eq 5). In eq 5, X equals either M for monomer or E for excimer.

$$i_X(t) = \sum_{i=1}^{n_{exp}} a_{Xi} \exp(-t/\tau_{Xi}) \qquad n_{exp} = 2, 3, \text{ or } 4 \qquad (5)$$

The monomer fluorescence decays were also fitted by eq 1, which was derived from the blob model. Equation 1 is a variation of the equations generally used to deal with micellar systems.[12] Due to the random copolymerization synthetic procedure, some PyMAAm monomers are expected to be incorporated into the polymer backbone next to one another. These nearby pyrene moieties form excimer on a subnanosecond time scale which is dealt with by using a light-scattering correction.[5,8] Equations 1 and 5 were convoluted with the instrument response function $L(t)$. The light-scattering correction was introduced by adding the instrument response function to the convolution product according to eq 6[13]

$$I_X(t) = i_X(t) \otimes L(t) + a_{scatt} L(t) \qquad (6)$$

where the symbol ⊗ indicates the convolution and a_{scatt} indicates the fraction of light-scattering correction being applied. The resulting function $I_X(t)$ was then compared with the experimental fluorescence decay, and the parameters of either eq 1 or 5 were optimized using the Marquardt−Levenberg algorithm.[14a]

The excimer decays were also fitted with eq 3. In eq 3, τ_D was fixed to equal τ_{E_3} obtained from the triexponential fits of the excimer fluorescence decays. The A_2, A_3 and A_4 values were taken from the results of the fits of the monomer decays with eq 1 and kept constant in the analysis. A general linear least-squares routine was used to fit the excimer fluorescence decays.[14b] The χ^2 parameter was optimized by applying a Golden section search to the lifetime τ_{E_0}.[14c]

Results

Steady-state fluorescence spectra were recorded for all PyPDMAAm polymer solutions in DMF, acetone, water, and acetone/water mixtures. Fluorescence measurements were all performed at low polymer and consequently low pyrene concentrations to prevent intermolecular pyrene excimer formation. The pyrene concentration of all the polymer solutions were determined by absorption measurements to be 3×10^{-6} M. Figure 1A shows the normalized spectra of the polymers PyPDMAAm in acetone with pyrene contents ranging from 15 to 350 μmol/g. The spectra were normalized at 374 nm, which corresponds to the 0−0 peak. Figure 1A shows that more excimer is being formed intramolecularly as the pyrene content of the polymer increases. Similar trends were observed for all solvents. The ratio of excimer to monomer, I_E/I_M, was calculated. Since the process of excimer formation is diffusion-controlled, the solvent viscosity (η(water, 24 °C) = 0.96 mPa·s, η(acetone, 24 °C) = 0.31 mPa·s) is taken into account by multiplying the ratio I_E/I_M by the solvent viscosity (η). The solvent viscosity of 15% acetone and 85% water (w/w, 15 acetone/85 water) mixture was measured with an Ubbelhode viscometer and found to be higher than that of water (η(15 acetone/85 water, 24 °C) = 1.23 mPa·s), and the viscosity of the 35% acetone and 65% water mixture (w/w, 35 acetone/65 water) was even higher (η(35 acetone/65 water, 24 °C) = 1.41 mPa·s). The product of $\eta \times I_E/I_M$ is plotted as a function of pyrene content in Figure 1B.

According to the Birks' scheme, the ratio $\eta I_E/I_M$ increases linearly with concentration for molecular pyrenes in a homogeneous solution.[6] When pyrene is covalently attached onto a polymer backbone, the ratio

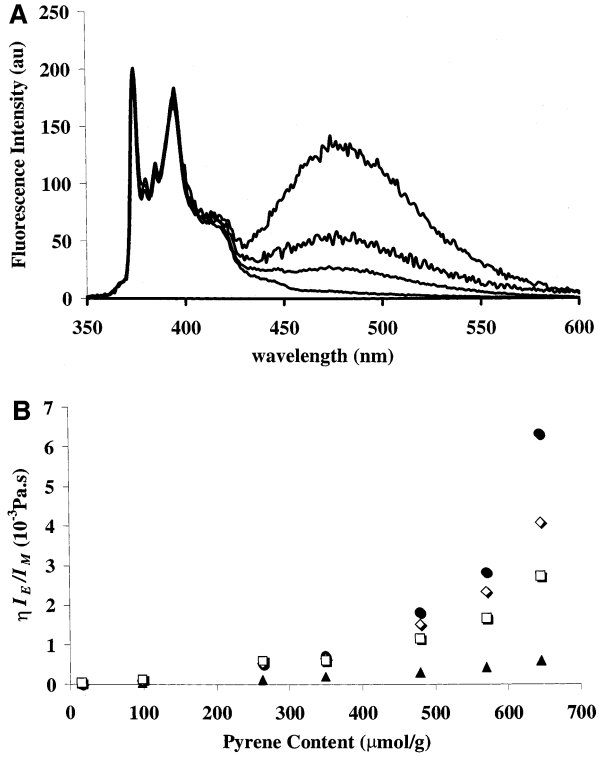

Figure 1. Samples excited at 344 nm: (A) fluorescence spectra of 15, 100, 185, and 350-PyPDMAAm in acetone (from bottom to top); (B) ratio $\eta I_E/I_M$ as a function of pyrene content, λ (μmol/g) (● in water, ▲ in acetone, □ in 35 acetone/65 water mixture, and ◇ in 15 acetone/85 water mixture). The pyrene concentration of these polymer solutions was 3×10^{-6} M.

$\eta I_E/I_M$ has been found to increase exponentially with pyrene content.[8] This trend is observed in Figure 1B for PyPDMAAm in all solvents. Figure 1B further indicates that the steep $\eta I_E/I_M$ increase is more pronounced for the polymer solutions in water at higher pyrene contents ($\lambda > 300$ μmol/g). This trend is due to the presence of aggregates of ground-state pyrenes in water.[7,15] Upon excitation, unassociated pyrenes will form excimer slowly via diffusion. On the other hand, ground-state pyrene dimers present in water form excimer instantaneously. The process of excimer formation is thus expected to be much more efficient in water than it is in acetone or DMF, resulting in a larger $\eta I_E/I_M$ value in water than in acetone for a given pyrene content. Intermediary trends were observed for the acetone/water mixtures.

The existence of pyrene-pyrene ground-state associations can be established qualitatively from UV−vis absorbance measurements and the analysis of the excimer fluorescence decays. When the 1-pyrenyl moiety is used to label a polymer, a broadening of the absorbance peak at 344 nm is observed upon pyrene aggregation.[7] The broadness of the peak is quantified by determining the ratio P_A of the absorbance at the peak at 344 nm to that of the nearest valley (P_A = Abs(peak)/Abs(valley)). The P_A value is close to 3.0 in the absence of associations and lower when associations are present. Figure 2 shows that this value equals 2.8 ± 0.1 for all the polymers in acetone, indicating little pyrene aggregation. The same trend is observed in DMF where the P_A value equals 2.9 ± 0.1. The P_A value is much lower in water, ranging from 2.1 for 15-PyPDMAAm to 1.4 for 650-PyPDMAAm in water. The decrease in P_A value with increasing pyrene content observed in water

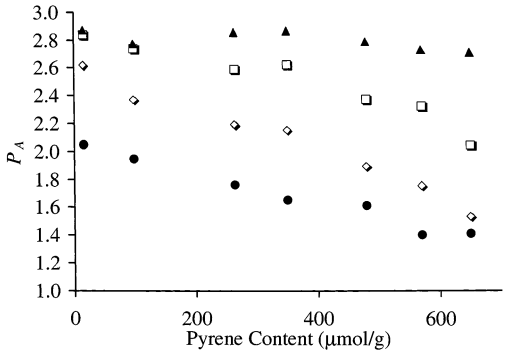

Figure 2. Peak-to-valley ratios (P_A) of the UV−vis absorption spectra of the PyPDMAAms at 344 nm (● in water, ▲ in acetone, □ in the 35 acetone/65 water mixture, and ◇ in the 15 acetone/85 water mixture). The pyrene concentration of these polymer solutions was 3×10^{-6} M.

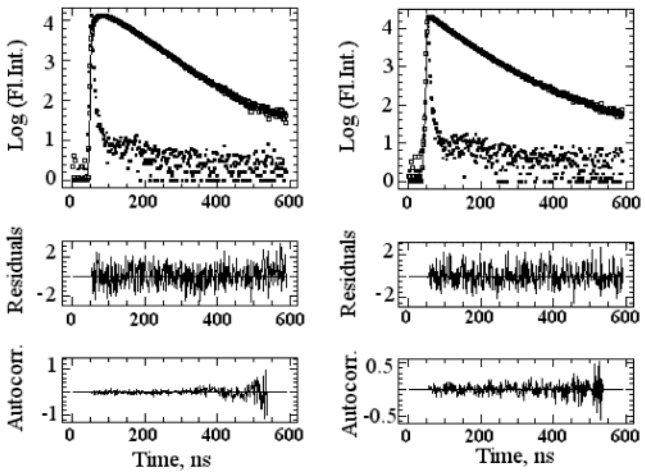

Figure 3. Excimer fluorescence decays of 350-PyPDMAAm in water (right) and acetone (left) (λ_{ex} = 344 nm, λ_{em} = 510 nm). The pyrene concentration of these polymer solutions was 3×10^{-6} M. The residuals and the autocorrelation function of the residuals are randomly distributed around 0.

indicates that more pyrenes aggregate for polymers with higher pyrene contents. When acetone is added to the water solution the amount of associations reduces with the increase of acetone content. In the 15 acetone/85 water mixed solvent, the P_A value ranged from 2.6 to 1.5, showing a decrease in the amount of associations, and in the 35 acetone/65 water mixed solvent the P_A value ranged from 2.8 to 2.0. These results clearly indicate that acetone in water reduces or "melts" the associations.

Similar conclusions can be drawn from the analysis of the excimer fluorescence decays. In an excimer fluorescence decay, the presence of a rise time is attributed to the formation of excimers by diffusional encounters between one excited pyrene and ground-state pyrenes. All the excimer decays were fitted with three exponentials yielding the rise time (τ_{E_1}), two decay times (τ_{E_2} and τ_{E_3}) and their corresponding preexponential weights (a_{E_1}, a_{E_2} and a_{E_3}). These are reported in Table S1 in the Supporting Information. Because of the presence of a rise time (cf. Figure 3), a negative amplitude (a_{E_1}) is obtained. The ratio

$$\xi = \frac{a_{E_1}}{a_{E_2} + a_{E_3}}$$

gives information about whether the excimers are formed by preassociation ($\xi = 0.0$) or by diffusional encounters ($\xi = -1.0$).[5b] The ratio ξ equaled -0.75 ± 0.07 in acetone and DMF and -0.08 ± 0.04 in water indicating large amounts of preassociated pyrenes in water but not in acetone and DMF. In the case of mixed solvents, the ξ ratio equaled -0.14 ± 0.06 and -0.38 ± 0.08 with 15 acetone/85 water and 35 acetone/65 water, respectively. The triexponential analysis of the excimer fluorescence decays shows that in the 15 acetone/85 water and 35 acetone/65 water mixtures, the amount of associations is intermediary between that in acetone and water.

Interestingly, the ξ ratio obtained from the triexponential analysis of the excimer fluorescence decays remained constant with pyrene content for all solvents considered. This behavior is different from that observed for the P_A values shown in Figure 2, where a downward trend is obtained with increasing pyrene content for any solvent that induces some pyrene associations. A priori, these observations are contradictory since the P_A measurements indicate increased levels of association with increased pyrene content, whereas the ξ ratios suggest that the level of association is independent of pyrene content. These differences arise from the nature of the techniques used. In an excimer fluorescence decay, only those pyrenes that produce excimer are accounted for. In a P_A measurement, all pyrenes present in the solution are monitored, even those which do not form any excimer. The contribution of the pyrenes which do not form any excimer is larger at low pyrene content and negligible at high pyrene content. Consequently their dependency on pyrene content affects the P_A measurements but not the ξ ratios.

Informative as they might be, the previous measurements do not provide any quantitative information about the level of association of these polymer/solvent systems. To this date, the procedure outlined in the Theory section is the only one which can yield this information for an AP where the associative pendants are made of pyrene dyes. This procedure was used toward the quantitative determination of the fractions f_{diff}, f_{free}, f_{E_0}, and f_D (cf. eq 4). First the lifetime (τ_M) of the unquenched pyrene attached onto the polymer backbone was determined from the monomer fluorescence decays of the 15-PyPDMAAm polymer. All monomer fluorescence decays were fitted with a sum of exponentials and the preexponential factors and decay times are reported in Table S2 in the Supporting Information. 15-PyPDMAAm has the lowest pyrene content and most of the pyrenes attached onto the polymer backbone exist as single isolated monomers which form hardly any excimer. The fits of the decays of 15-PyPDMAAm yielded a long decay time with a minimum 86% contribution of the preexponential weights. This long decay time was attributed to τ_M and was found to equal 256 ns in acetone, 255 ns in 35 acetone/65 water, 250 ns in 15 acetone/85 water, 245 ns in water, and 220 ns in DMF.

In each solvent, the parameters f, k_{blob}, $\langle n \rangle$, and k_e[blob] were retrieved from the analysis of the monomer fluorescence decays with eq 1. The χ^2 were smaller than 1.30, the residuals and autocorrelation function of the residuals were randomly distributed around zero indicating good fits of the fluorescence decays. The f, k_{blob}, $\langle n \rangle$, k_e[blob], and χ^2 values are listed in Table S3 in the Supporting Information. Within experimental error, k_{blob} and k_e[blob] were found to remain constant with pyrene content, and their average values have been listed in Table 2.

Table 2. Summary of the Parameters Retrieved by the Blob Model Analysis of the Monomer Fluorescence Decays

solvent	η (10^3 Pa·s)	k_{blob} (10^7 s^{-1})	N_{blob}	k_e[blob] (10^6 s^{-1})
water	0.89	1.9 ± 0.0	19 ± 1[a]	6.1 ± 1.5
15% w/w acetone/ 85% w/w water	1.23	1.4 ± 0.2	25 ± 2[a]	5.5 ± 0.7
35% w/w acetone/ 65% w/w water	1.41	1.1 ± 0.1	31 ± 2[a]	4.8 ± 0.5
acetone	0.31	0.9 ± 0.1	60 ± 6	5.3 ± 0.1
DMF	0.79	1.1 ± 0.1	26 ± 1	6.9 ± 0.9

[a] For these systems, the pyrene ⇔ quencher equivalence does not exist due to the presence of hydrophobic associations ($f_{agg} > 0.0$). $\langle n \rangle$ does not equal the number of pyrene per blob, and the N_{blob} value recovered in these solvents is not accurate.

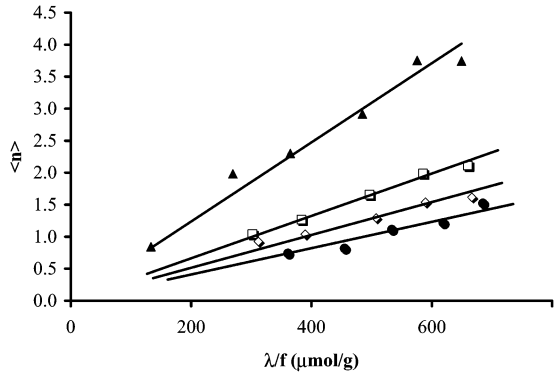

Figure 4. Plot of $\langle n \rangle$ vs λ/f where the parameters $\langle n \rangle$, and f have been retrieved from the analysis of the monomer fluorescence decays ($\lambda_{ex} = 344$ nm, $\lambda_{em} = 375$ nm) with eq 1 (● in water, ▲ in acetone, □ in the 35 acetone/65 water mixture, and ◇ in the 15 acetone/85 water mixture).

The average number of quenchers per blob, $\langle n \rangle$, yielded the size of the blob (N_{blob}) using eq 7.[8] In eq 7, x is the mole fraction of pyrene labeled acrylamide units in the copolymer, and 285 and 99 represent the molar masses of the pyrene labeled acrylamide and *N*,*N*-dimethylacrylamide. In each solvent, N_{blob} remains constant with pyrene content within experimental error and the average value is listed in Table 2. In each solvent, the average number of quenchers per blob ($\langle n \rangle$) and the product $k_{blob}\langle n \rangle$ increase linearly with the corrected pyrene content (λ/f) as shown in Figures 4 and 5, respectively. The correction $1/f$, where f is the fraction of pyrene monomers that do form excimer by diffusion (cf. eq 1), accounts for the fact that some domains of the polymer coil are poor in pyrene and do not contribute to the process of excimer formation.[8] Except for 100-PyPDMAAm, f is usually close to 1.0 and the ratio λ/f takes a value, which is close to the nominal pyrene content of the polymer (λ):

$$N_{blob} = \frac{\langle n \rangle}{(\lambda/f)(285x + 99(1 - x))} \qquad (7)$$

The trends exhibited in each solvent by the parameters k_{blob}, $\langle n \rangle$, k_e[blob], and N_{blob} as well as by the product $k_{blob}\langle n \rangle$ are expected according to the blob model framework and discussed in more detail in the following section. At this stage, all the parameters (i.e., k_{blob}, $\langle n \rangle$, and k_e[blob]) relevant to excimer formation by diffusion have been obtained. Equation 3 was used to fit the

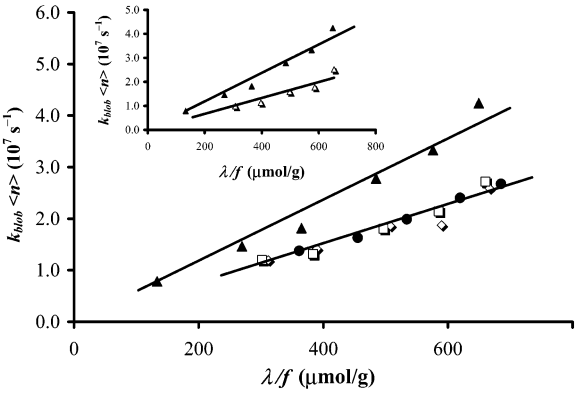

Figure 5. Plot of $k_{blob}\langle n\rangle$ vs λ/f where the parameters k_{blob}, $\langle n\rangle$, and f have been retrieved from the analysis of the monomer fluorescence decays (λ_{ex} = 344 nm, λ_{em} = 375 nm) with eq 1 for water, acetone and mixtures of the two (● in water, ▲ in acetone, □ in the 35 acetone/65 water mixture and ◇ in the 15 acetone/85 water mixture). The inset shows the same plot for polymers in acetone (▲) as compared with DMF (△).

excimer decays. The parameters k_{blob}, $\langle n\rangle$, and k_e[blob] retrieved from the monomer decay analysis were fixed in eq 3. Initially the excimer decays were fitted assuming that no long-lived excited dimers were present (i.e., $[D^*]_0 = 0$). The fits were poor at the longer times. The presence of a long-lived component in the excimer decays is confirmed by carrying out a triexponential fit (results listed in Table S1 in the Supporting Information). The excimer fluorescence decays had long decay times (τ_{E_3}) of 106 ± 15, 112 ± 21, 128 ± 19, 120 ± 15, and 133 ± 26 ns in water, the 15 acetone/85 water mixture, the 35 acetone/65 water mixture, acetone, and DMF, respectively. These long decay times were recovered with lesser accuracy because the contributions of their preexponential weight were small. Although their presence in the decays was small, they had to be taken into account because the biexponential fits were poor. As a consequence, the lifetime of the long-lived excited dimers τ_D was arbitrarily fixed in the analysis of the excimer decays with eq 3 to equal the values τ_{E_3} retrieved from the triexponential fits. On the basis of the long decay times found in the triexponential fits of the excimer decays, τ_D values of 100, 110, 125, 120, and 130 ns were chosen for the analysis of the excimer decays in water, the 15 acetone/85 water mixture, the 35 acetone/65 water mixture, acetone, and DMF, respectively. The fits were carried out with eq 3 and found to be good. The excimer lifetime τ_{E_0} and the fractions of all fluorescent species present in solution were determined for each polymer/solvent pair. The τ_{E_0} values equaled 52.5 ± 2.5, 55.7 ± 2.7, 55.0 ± 2.0, 51.7 ± 2.3, and 53.8 ± 2.2 ns in water, the 15 acetone/85 water mixture, the 35 acetone/65 water mixture, acetone, and DMF, respectively. These values are reasonable for the lifetime of the pyrene excimer.[6] They are listed in Table S4 in the Supporting Information. The fraction of aggregated pyrene pendants (f_{agg}) is given by the sum of f_{E_0} and f_D. It is plotted in Figure 6 for all the solvents considered.

Discussion

The kinetics of excimer formation for dilute solutions of PyPDMAAm with different pyrene contents were investigated using a blob model. For each solvent, the parameters retrieved from the monomer fluorescence decay analysis (i.e., k_{blob}, $\langle n\rangle$, k_e[blob]) can be shown to

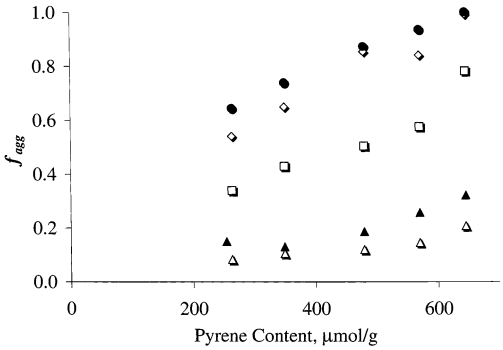

Figure 6. Fraction of associated pyrenes for the polymers studied (● in water, ▲ in acetone, □ in the 35 acetone/65 water mixture, ◇ in the 15 acetone/85 water mixture, and △ in DMF).

be consistent within the framework of the blob model. However comparison of the results obtained with different solvents requires a thorough understanding of the physical meaning of the blob model parameters. A description of how k_{blob} and $\langle n\rangle$ are expected to behave is provided hereafter.

The rate of excimer formation by diffusion between one excited pyrene and one ground-state pyrene located inside the same blob (k_{blob}) is a pseudo-unimolecular rate constant. In fact, k_{blob} is the product of the rate constant of diffusion-controlled encounter with the equivalent concentration of one ground-state pyrene inside one blob, i.e.

$$k_{blob} = k \times \frac{1}{V_{blob}}$$

The rate constant k is inversely proportional to the solvent viscosity η ($k \propto \eta^{-1}$).[16] As the solvent viscosity increases, a smaller volume is being probed by an excited pyrene so that V_{blob} is also inversely proportional to the solvent viscosity ($V_{blob} \propto \eta^{-1}$). The consequence is that k_{blob} is not expected to depend on solvent viscosity.

$$k_{blob} = k \times \frac{1}{V_{blob}} \propto \frac{\eta^{-1}}{\eta^{-1}}$$

Experimental support for this conclusion is presented in a forthcoming article.[19] This result is unexpected because the rate constant of excimer formation by diffusion in numerous other systems exhibiting restricted geometries must be corrected for medium viscosity when comparisons between systems are being made.[20] This is because these systems have well-defined boundaries which do not change with viscosity. In this respect, the blob model is unique since the boundary of the restricted volume where excimer formation takes place evolves with solvent viscosity.

Although k_{blob} does not depend on solvent viscosity, the rate of excimer formation by diffusion k_{blob} is inversely proportional to the blob volume ($k_{blob} \propto 1/V_{blob}$). This statement is similar to the one made for micellar systems for which the pseudo-unimolecular rate of quenching inside a micelle is inversely proportional to the micellar volume.[21] The parameter $\langle n\rangle$ is the average number of quencher per blob where a quencher is either a ground-state pyrene or a ground-state pyrene aggregate. Consequently the product $k_{blob}\langle n\rangle$ is proportional to $\langle n\rangle/V_{blob}$, which represents the local quencher concentration inside the polymer coil.

Water, Acetone and Mixed Solvents. Figure 5 shows that the local quencher concentration ($k_{blob}\langle n\rangle$) obtained by fluorescence increases linearly with the corrected pyrene content (λ/f) obtained by UV−vis absorbance. For each solvent, k_{blob} remains constant with pyrene content and its values are listed in Table 2. Since k_{blob} is inversely proportional to V_{blob}, the quantity V_{blob} remains constant with pyrene content of the polymer for a given solvent. As the pyrene content increases, more pyrenes fill the blobs and the average number of quencher per blob ($\langle n\rangle$) increases linearly with the corrected pyrene content (cf. Figure 4). The fact that the blob model yields reasonable trends even in water is remarkable due to the presence of hydrophobic pyrene associations which induce a hydrophobic collapse of the polymer coil.

The plots of $k_{blob}\langle n\rangle$ vs (λ/f) shown in Figure 5 overlap for water and for the 15 acetone/85 water and 35 acetone/65 water mixtures. In water, most pyrene groups are associated (cf. Figure 6) and the quenchers are mostly aggregates of ground-state pyrenes. The pyrene ⇔ quencher equivalence does not hold in water or the acetone/water mixtures because significant associations between pyrenes lead to the following relationship:

$$[\mathrm{Py}]_{loc} >> [Q]_{loc} = \frac{\langle n\rangle}{V_{blob}}$$

As a matter of fact, the local quencher concentration ($[Q]_{loc}$) is related to the local pyrene concentration ($[Py]_{loc}$) according to the following relationship:

$$[Q]_{loc} = [\mathrm{Py}]_{loc}\left(1 - f_{agg} + \frac{f_{agg}}{N_{agg}}\right) \propto k_{blob}\langle n\rangle \qquad (8)$$

where N_{agg} represents the average number of pyrene units per pyrene aggregate. According to eq 8 and assuming a hypothetical N_{agg} of 20, $[Q]_{loc}$ will be 20 times smaller than $[Py]_{loc}$ if f_{agg} equals 1.0. Thus, knowledge of the level of association becomes critical when comparing the local quencher concentration inside the polymer coil in different solvents. The pyrene ⇔ quencher equivalence exists only in those solvents where f_{agg} is close to 0, i.e., acetone and DMF in the present study (cf. Figure 6). The pyrene ⇔ quencher equivalence is also required for the determination of N_{blob}. Since eq 7 used to calculate N_{blob} requires the average number of pyrene per blob, it can be used only for those solvents where f_{agg} is close to zero, i.e., none of the solvents inducing pyrene associations. Nevertheless, it is worth noting that the determination of the fractions f_{diff}, f_{free}, f_{E_0}, and f_D is not affected by the presence of pyrene aggregates, despite the fact that the meaning of the parameters retrieved from the blob model might be affected by it.

Water being a poor solvent for pyrene, addition of water to the acetone solutions leads to the formation of pyrene aggregates. This was confirmed *qualitatively* by UV−vis absorbance measurements and from the analysis of the excimer rise time. This is confirmed *quantitatively* in Figure 6, where f_{agg} increases with increasing water content. For a given solvent, f_{agg} increases also with the pyrene content of the polymer indicating increased pyrene associations. This agrees with the qualitative P_A trends obtained by UV−vis absorbance (cf. Figure 2). In water, f_{agg} equals 1.0 only for the highest pyrene contents investigated in this study. Interestingly polymers with lower pyrene contents have an f_{agg} value which is lower than 1.0. For 265PyPDMAAm in water, only 64% of all pyrene groups are associated. A similar result (58%) has been obtained for two pyrene-labeled hydrophobically modified alkali swellable emulsion copolymers with pyrene contents of 42 and 65 μmol/g.[5b]

Addition of acetone to the aqueous polymer solutions melts the pyrene aggregates and frees the polymer chain, the excited pyrene monomers probe a larger volume, and k_{blob} decreases (cf. Table 2). Since the addition of acetone melts the pyrene aggregates, more pyrene groups are available to act as quencher and the number of quenchers ($\langle n\rangle$) populating the larger blobs increases. This is observed in Figure 4. Multiplying the decreasing k_{blob} by the increasing $\langle n\rangle$ results in a constant local quencher concentration and within experimental error, no difference is observed for the plots of $k_{blob}\langle n\rangle$ vs (λ/f) in water and the 15 acetone/85 water and 35 acetone/65 water mixtures.

Since the k_{blob} values in acetone and the 35 acetone/65 water mixture are equal within experimental error, an excited pyrene probes a similar volume in both solvents. However, f_{agg} is much larger in the 35 acetone/65 water mixture than in acetone (cf. Figure 6). Switching the solvent from the 35 acetone/65 water mixture to acetone melts the remaining pyrene aggregates. Thus, acetone generates more quenchers which can distribute themselves among blobs which have similar sizes in acetone and in the 35 acetone/65 water mixture. Consequently the local quencher concentration ($k_{blob}\langle n\rangle$) is larger in acetone than in water and the 15 acetone/85 water and 35 acetone/65 water mixtures.

Acetone and DMF. The blob model has been used to determine the fraction of associated pyrenes of different PyPDMAAms in four solvent systems so far. Figure 6 shows that f_{agg} is much smaller in acetone than in water but also, that it is smaller than in the acetone/water mixtures, as expected. It equals 0.21 ± 0.07 in acetone, which indicates that 21% of all pyrenes are preassociated, even in acetone which is a good solvent for pyrene according to the P_A values shown in Figure 2. Two reasons can be evoked to rationalize the presence of residual pyrene associations in acetone. First PyPDMAAm is made by radical copolymerization and PyMAAm is incorporated randomly into the polymer backbone. If some PyMAAm monomers are incorporated next to each other, they will form excimer instantaneously and cannot be distinguished from pyrene ground-state aggregates. Consequently the random incorporation of PyMAAm can result in a nonzero value of f_{agg}. Second poor solvent quality toward the polymer backbone can also lead to nonzero f_{agg} values. A poor solvent will yield a collapsed polymer coil where the pyrenes are closer to one another, inducing the formation of pyrene aggregates.

The second viral coefficients (A_2) were measured by light-scattering for all PyPDMAAms in acetone, and they are listed in Table 3. Interestingly, A_2 decreases with increasing pyrene content, which indicates that the incorporation of pyrene into the polymer decreases the polymer−solvent interaction parameter and thus also the solubility of the copolymer in acetone. According to the A_2 values, acetone switches from a mediocre solvent for PyPDMAAm at low pyrene contents to a bad solvent at pyrene contents larger than 500 μmol/g. Being at best

Table 3. Second Viral Coefficients and Intrinsic Viscosity Obtained for the PyPDMAAm Polymers in Acetone and DMF

	A_2 (10^{-4} cm^3·mol·g^{-2})		[η] (cm^3·g^{-1})	
	DMF (±10%)	acetone[b] (±20%)	DMF	acetone
PDMAAm[a]	2.1	2.8	21.8 ± 0.1	21.2 ± 0.1
100PyPDMAAm		0.9		
265PyPDMAAm	2.3	0.9	36.5 ± 0.2	27.6 ± 0.2
350PyPDMAAm		0.7		
480PyPDMAAm	1.6	−0.0		
570PyPDMAAm		−0.5		
645PyPDMAAm	1.6	−0.8	17.2 ± 0.1	11.5 ± 0.3

[a] In water, PDMAAm has an A_2 of 3.1×10^{-4} cm^3·mol·g^{-2} and [η] of 30.7 ± 0.2 cm^3·g^{-1}. [b] Larger errors are associated with acetone due to the higher volatility of the solvent.

a mediocre solvent for PyPDMAAm, acetone could yield artificially high levels of association. To monitor the effects of solvent quality on f_{agg}, a new set of experiments were completed in DMF which was expected to be a better solvent for PyPDMAAm. This was confirmed by static light-scattering which yielded A_2 values which were consistently larger in DMF than in acetone (cf. Table 3). Furthermore, the A_2 coefficients were positive regardless of the pyrene content for the four PyPDMAAms studied in DMF. That acetone is a mediocre solvent and DMF a good one for the PyPDMAAms was confirmed by carrying out intrinsic viscosity ([η]) measurements. The pyrene-labeled polymers yield [η] values, which were found to be consistently and significantly smaller in acetone than in DMF (cf. Table 3), further confirming that the PyPDMAAm coil is more expanded in DMF than in acetone.

Within experimental error, the parameters k_{blob}, N_{blob}, k_e[blob], and f_{agg} retrieved for the PyPDMAAms in DMF remained constant with pyrene content and equaled $1.1 \pm 0.1 \times 10^7$ s^{-1}, 26 ± 1, $6.9 \pm 0.9 \times 10^6$ s^{-1} and 0.13 ± 0.05. Changing the solvent from acetone (mediocre solvent for PyPDMAAm) to DMF (good solvent for PyPDMAAm) yielded a lower level of association as expected, but f_{agg} remained larger than 0.0 in DMF. The remaining "residual" association observed in DMF must be due to the random incorporation of short PyMAAm stretches into the polymer backbone. Although f_{agg} does not equal 0.0 in DMF and acetone, it is rather small in both solvents so that the quencher ⇔ pyrene equivalence can be assumed to hold in both solvents at first approximation. Consequently $\langle n \rangle$ represents the number of pyrene per blob and the values retrieved for N_{blob} are not expected to be severely affected by the presence of residual pyrene ground-state aggregates. The blob size N_{blob} was found to be 2.3 ± 0.2 times larger in acetone than in DMF, whereas the blob volume does not change much between acetone and DMF (k_{blob}[for acetone] ≈ k_{blob}[for DMF]). Thus, the polymer coil is less dense in DMF than in acetone, as expected since DMF is a better solvent for PyPDMAAms. Since the chains are stretched in DMF, the pyrenes are far apart resulting in a lower f_{agg} value in DMF than in acetone.

Relationship with Other Works. Hydrophobically modified PDMAAms (HM-PDMAAm) with hydrophobes incorporated along the polymer backbone belong to the category of APs described as multisticker chains.[22] In the semidilute and entangled concentration regime, each chain is held in place by two types of physical ties, namely the entanglements of the polymer chain and the hydrophobic aggregates. Under stress, a HM-PDMAAm chain can relax by reptating out of its tube only when it has been released from all its hydrophobic ties. The theory dealing with the viscoelastic behavior of these polymeric solutions was developed by Leibler et al. and it combines reptation with the notion that the chain motion is slowed by stickers involved into transient associations.[23] One ubiquitous parameter in Leibler et al. theory is p, the fraction of stickers engaged in an association, referred to as f_{agg} in this study. Candau et al. have shown that several scaling behaviors predicted by the Leibler et al. model are well-obeyed.[22b,c] However none of these measurements can access the p parameter in situ as fluorescence measurements can do with f_{agg}. The ability to determine the f_{agg} parameter by fluorescence should open new research venues for the characterization of the viscoelastic behavior of multisticker chains in the semidilute and entangled concentration regime.

Recently HM-PDMAAms have been shown to form thermally reversible coacervates.[24] This property leads to potential applications for HM-PDMAAm in separation technology[24] and in drug delivery systems[25a] among others.[25] HM-PDMAAms have been synthesized with *N*-phenylacrylamides,[24] *N*-[1-(1-pyrene)octadecyl]acrylamide,[26a] *N*-octadecylacrylamide,[26b] *N*-dodecylmethacrylamide,[26b] and 2-(*N*-ethylperfluorooctanesulfonamido)-ethyl acrylate as hydrophobes.[26c] The rheological properties of HM-PDMAAms have been examined in the three later cases. Of these, only those polymers containing perfluorinated alkyl side groups exhibit strong associating behavior at less than 1.5 mol % hydrophobic content and molecular masses on the order of 10^6 g/mol.[26e] HM-PDMAAms containing hydrocarbon alkyl chains exhibit some associating behavior as well but at higher concentration, with higher hydrophobic content (2.8 and 6.5 mol %) with lower molecular masses (10^4 g/mol).[26c] The underlying feature of all these systems resides in the associative power exhibited by the hydrophobes of the HM-PDMAAms. The determination of f_{agg} as a function of the chemical structure of the HM-PDMAAms should provide valuable information toward the design of improved thermally reversible coacervates. If the dye pyrene can be covalently attached onto the hydrophobe, the present study demonstrates that f_{agg} can be determined by fluorescence.

Conclusions

The hydrophobic chromophore pyrene has been covalently attached onto a water-soluble polymer backbone, poly(*N*,*N*-dimethylacrylamide). In water, hydrophobic associations between the pyrene hydrophobes take place. Their presence was established qualitatively by monitoring two well-established spectroscopic effects, namely the broadening of the absorbance peak at 344 nm and the disappearance of a rise time in the excimer decays. Upon addition of a less polar solvent like acetone, the pyrene aggregates melt. Using a blob model, the level of association of the pyrene hydrophobes could be determined quantitatively. In a given solvent, f_{agg} increases with pyrene content and decreases upon addition of an organic solvent like acetone which melts the hydrophobic aggregates. Switching the solvent from acetone (a mediocre solvent for PyPDMAAm) to DMF (a good solvent for PyPDMAAm) further reduces f_{agg} since the polymer coil expands and the pyrene groups are more isolated.

In this work, the determination of f_{agg} demanded the knowledge of how the pyrene pendants diffusionally

encounter. This was accomplished by applying the blob model. The diffusion-controlled encounters between pyrenes could be analyzed in a variety of solvents having different solvating properties. DMF is a good solvent for the polymer backbone and the pyrene pendants. Acetone is a good solvent for the pyrene pendants, but a poor one for the polymer backbone. Water and the acetone/water mixtures were good solvents for the polymer backbone but bad ones for the pyrene pendants. These solvent/polymer combinations cover any possible situation which can be encountered with this series of pyrene-labeled PDMAAms. Regardless of the polymer/solvent combination investigated, the blob model gave a quantitative description of the polymeric system which was always in agreement with the qualitative information known about the system (solvent quality, hydrophobic associations).

Acknowledgment. The authors thank the NSERC for generous funding.

Supporting Information Available: Figure showing plots the ^{1}H NMR experiments following the incorporation of PyDMAAm into the copolymer as a function of conversion and tables listing the parameters retrieved from the fits of the fluorescence decays. This material is available free of charge via the Internet at http://pubs.acs.org.

References and Notes

(1) Glass, J. E. Hydrophilic Polymers. Performance with Environmental Acceptability. *Adv. Chem. Ser.* **1996**, *No. 248*. Schulz, D. N.; Glass, J. E. Polymers as Rheology Modifiers. *ACS Symp. Ser.* **1989**, *No. 462*. Glass, J. E. Polymers in Aqueous Media. *Adv. Chem. Ser.* **1989**, *No. 223*.

(2) Annabale, T.; Buscall, R.; Ettelaie, R.; Whittlestone, D. *J. Rheol.* **1993**, *37*, 695−726. Jenkins, R. D.; DeLong, L. M.; Bassett, D. R. Hydrophilic Polymers. Performance with Environmental Acceptability. *ACS Symp. Ser.* **1996**, *No. 248*, 425−447.

(3) Yekta, A.; Duhamel, J.; Adiwidjaj, H.; Brochard, P.; Winnik, M. A. *Langmuir* **1993**, *9*, 881−883. Yekta, A.; Xu, B.; Duhamel, J.; Adiwidjaja, H.; Winnik, M. A. *Macromolecules* **1995**, *28*, 956−966. Winnik, M. A.; Yekta, A. *Curr. Opin. Colloid Interface Sci.* **1997**, *2*, 424−436.

(4) English, R.; Gulati, H. S.; Jenkins, R. D.; Khan, S. A. *J. Rheol.* **1997**, *41*, 427−444. Tirtaatmadja, V.; Tam, K. C.; Jenkins, R. D. *Macromolecules* **1997**, *30*, 1426−1433. Vittadello, S. T.; Biggs, S. *Macromolecules* **1998**, *31*, 7691−7697. Noda, T.; Hashidzume, A.; Morishima, Y. *Langmuir* **2001**, *17*, 5984−5991.

(5) (a) Vangani, V.; Drage, J.; Mehta, J.; Mathew, A. K.; Duhamel, J. *J. Phys. Chem. B* **2001**, *105*, 4827−4839. (b) Prazeres, T. J. V.; Beingessner, R.; Duhamel, J.; Olesen, K.; Shay, G.; Bassett, D. R. *Macromolecules* **2001**, *34*, 7876−7884.

(6) Birks, J. B. *Photophysics of Aromatic Molecules*; Wiley: New York, 1970; pp 301−371.

(7) Winnik, F. M. *Chem. Rev.* **1993**, *93*, 587−614.

(8) Mathew, A. K.; Siu, H.; Duhamel, J. *Macromolecules* **1999**, *32*, 7100−7108.

(9) In previous publications from this laboratory, the rate of excimer formation inside a blob was referred to as k_{diff}. It was pointed out by an unknown reviewer that since the process of excimer formation inside a blob does not depend on viscosity, the choice of k_{diff} as a mathematical symbol was not appropriate and confusing to the reader. Consequently, we have been using the symbol k_{blob} instead of k_{diff}.

(10) Piçara, S.; Gomes, P. T.; Martinho, J. M. G. *Macromolecules* **2000**, *33*, 3947−3950, Reynders, P.; Dreeskamp, H.; Kühnle, W.; Zachariasse, K. A. *J. Phys. Chem.* **1987**, *91*, 3982−3992.

(11) Kratochvíl, P. *Classical Light Scattering from Polymer Solutions*; Elsevier: Amsterdam, 1987; Chapter 5.

(12) Infelta, P. P.; Gratzel, M.; Thomas, J. K. *J. Phys. Chem.* **1974**, *78*, 190−195.

(13) Demas, J. N. *Excited-State Lifetime Measurements*; Academic Press: New York, 1983; p 134.

(14) Press, W. H.; Flannery, B. P.; Teukolsky, S. A.; Vetterling, W. T. *Numerical Receipes. The Art of Scientific Computing (Fortran Version)*; Cambridge University Press: Cambridge, England, 1992: (a) pp 523−528; (b) pp 509−513; (c) p 282.

(15) Lee, S.; Duhamel, J. *Macromolecules* **1998**, *31*, 9193−9200.

(16) The relationship $k \propto \eta^{-1}$ assumes that the Stokes−Einstein relationship holds. However the relationship $k \propto \eta^{-a}$ has been found experimentally where the value of a depends on the solute and solvent molecules investigated.[17] The Stokes−Einstein relationship considers small spherelike molecules moving freely in solution. Although pyrenes attached onto a polymer backbone do not move freely in the solution, the rate of excimer formation has been shown to depend on the inverse of the solvent viscosity for pyrenes attached at both ends of a poly(ethylene oxide).[18] At this stage of our study, we assume that the $k \propto \eta^{-1}$ relationship holds to describe the encounters between pyrenes randomly attached onto the PDMAAm backbone.

(17) Olea, A. F.; Thomas, J. K. *J. Am. Chem. Soc.* **1988**, *110*, 4494−4502.

(18) Cheung, S.-T.; Winnik, M. A.; Redpath, A. E. C. *Makromol. Chem.* **1982**, *183*, 1815−1824.

(19) Kanagalingam, S.; Spartalis, J.; Cao, T.-M.; Duhamel, J. *Macromolecules*, in press.

(20) When pyrene is dissolved in a surfactant solution, excimer forms inside the surfactant micelle. When a monodisperse polymer is end-labeled with pyrene, excimer forms within the volume of the polymer coil. In these two examples, the volume where excimer is formed is well-defined.

(21) Gösele, U.; Klein, U. K. A.; Hauser, M. *Chem. Phys. Lett.* **1979**, *68*, 291−295.

(22) (a) Volpert, E.; Selb, J.; Candau, F. *Macromolecules* **1996**, *29*, 1452−1463. (b) Candau, F.; Regalado, E. J.; Selb, J. *Macromolecules* **1998**, *31*, 5550−5552. (c) Regalado, E. J.; Selb, J.; Candau, F. *Macromolecules* **1999**, *32*, 8580−8588.

(23) Leibler, L.; Rubinstein, M.; Colby, R. H. *Macromolecules* **1991**, *24*, 4701−4707.

(24) Miyazaki, H.; Kataoka, K. *Polymer* **1996**, ***37***, 681−685.

(25) (a) Yeh, P.-Y.; Kopeèkovâ, P.; Kopeèek, J. *J. Polym. Sci., Part A: Polym. Chem.* **1994**, *32*, 1627−1637. (b) Atherton, E.; Clive, D. L. J.; Sheppard, R. C. *J. Am. Chem. Soc.* **1975**, *97*, 6584−6585. (c) Kondo, S.; Nakashima, N.; Hado, H.; Tsuoa, K. *J. Polym. Sci., Part A: Polym. Chem.* **1990**, *28*, 2229−2232.

(26) (a) Uemura, Y.; McNulty, J.; Macdonald, P. M. *Macromolecules* **1995**, *28*, 4150−4158. (b) Guillaumont, L.; Bokias, G.; Iliopoulos, I. *Macromol. Chem. Phys.* **2000**, *201*, 251−260. (c) Xie, X.; Hogen-Esch, T. E. *Macromolecules* **1996**, *29*, 1734−1745.

MA0207428